01 Apr 2013

# Quantum Network Theory of Computing with Respect to Entangled Flux Qubits and External Perturbation

C. A. Cain

Cheng-Hsiao Wu
*Missouri University of Science and Technology*, chw@mst.edu

JOURNAL OF APPLIED PHYSICS **113**, 154309 (2013)

# Quantum network theory of computing with respect to entangled flux qubits and external perturbation

C. A. Cain and C. H. Wu[a)]
*Department of Electrical and Computer Engineering, Missouri University of Science and Technology, 301 W 16th St., Rolla, Missouri 65409, USA*

(Received 29 November 2012; accepted 1 April 2013; published online 17 April 2013)

In this work, we attempt to show the differences between traditional qubit-based spintronic methodology for quantum computation and the possible ballistic quantum network implementations. Flux qubits can be considered topologically similar to the persistent currents possessed as the angular momentum in Aharonov-Bohm loops, which can be coupled and thus entangled together. Since entanglement is guaranteed for coupled quantum networks, starting from a point-contacted situation, we first investigate how varying the degree of entanglement strength can affect the superposition of the four possible states for two isolated flux qubits being brought together. In general, the superposition is destroyed once the degree of entanglement is altered from the point-contact situation. However, we show that for a specific network with maximum entanglement, a Bell state situation can be produced. We then examine the effects of varying the external perturbation strength on the readout capability in quantum networks by changing the coupling strength through the cross-sectional area ratio. From the analysis of our results, we are persuaded to believe that two universally accepted components for quantum computing are not valid in the quantum network approach: the need of a weak perturbation for measurement of computational results and the requirement of fixed entanglement among qubits. We show there is an interplay between the strength of the entanglement and that of the external perturbation for high-fidelity classical readouts. © *2013 AIP Publishing LLC* [http://dx.doi.org/10.1063/1.4801807]

## I. INTRODUCTION

Quantum computing has been investigated extensively by many researchers founded on the qubit-based concept.[1–15] In the standard qubit formalism for a particle such as an electron, the state of the qubit can be written as the linear combination of the eigenstates of the Pauli spin matrix along the rotational (typically z) axis

$$S_z = \frac{\hbar}{2}\begin{bmatrix} 1 & 0 \\ 0 & -1 \end{bmatrix}, \quad (1)$$

with normalized eigenstates $\{(1,0),(0,1)\}$. In quantum network theory,[16–21] it is possible to extend the notion of a flux qubit to Aharonov-Bohm (AB) rings based on the angular momentum concept. The typical spin-up/spin-down eigenstates can be considered as the clockwise (CW)/counter-clockwise (CCW) circulating persistent currents flowing in an AB loop network, as shown in Fig. 1. Hence for a single isolated AB ring, the CW or CCW angular momentum superposition exists periodically with a period of $hc/e$ or $\Phi_0$. For example in Fig. 1 at $\Phi = \pm 0.5\Phi_0$ or 0, the persistent current will discontinuously switch between the global maximum and minimum. This always occurs at the Brillouin zone boundary or a Fermi level crossing between bonding and anti-bonding states. Therefore, the AB ring is similar to an atom whose angular momentum vector exhibits the switching of the eigenstates because the current oscillation is equivalent to a chain of coupled harmonic oscillator waves.

For a single qubit, the flux model for an AB ring seems to fit the traditional quantum computing concept. When two such isolated AB rings are entangled with each other by sharing a center common path, there are now two possible fluxes which can penetrate each loop, denoted by $\phi_1$ and $\phi_2$, with the flux periodicity deviating from the elementary flux quanta accordingly.[23] There is now an interaction along this channel between the two partial waves embedded in each ring, and hence, the Brillouin zone is two-dimensional. For quantum computing purposes, any ring-to-ring entanglement is supposed to provide the four possible spin pairings for parallel computation, which corresponds to the parallel execution of Boolean algebra addition for two values, typically called a half-adder. The two point-contacted AB rings (Fig. 2(a)) can fit into this picture with the superposition condition unaltered. However the ring-to-ring interaction, which can be arbitrarily and lithographically imposed (Fig. 2(b)), may or may not leave the superposition condition intact even if we allow the shift of applied flux at the superposition region. Second, the readout of the computation from the qubit concept requires that the external perturbation be very weak and brief as not to alter the state of the system's four spin pairing condition. In this paper, we show those two conditions are not valid from the quantum network theory. We describe in Sec. II how varying the entanglement strengths may change the existence of superposition for the four pairings. In essence, it depends on the ring-to-ring interaction (internal coupling) that is physically imposed on the system. Even if the entanglement between two AB rings manages to preserve the superposition at an altered flux period, any form

a)Electronic mail: chw@mst.edu

 

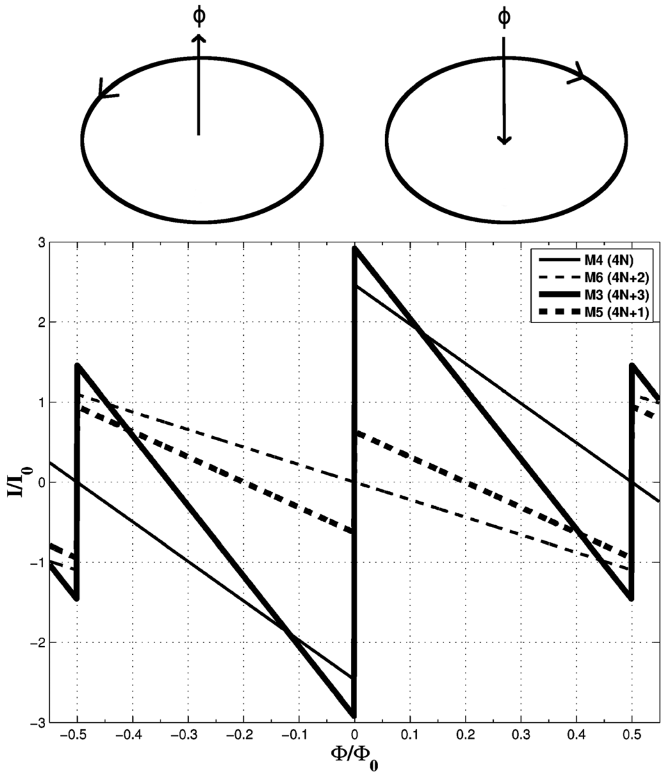


FIG. 1. Single isolated AB ring whose angular momentum state is in a superposition. At zero flux, there is an overlap at $E_f$ between bonding and anti-bonding states which causes this, with the other case being the zone boundary. There are four possible groups, $M = 4N$, $4N + 2$, $4N + 1$, and $4N + 3$, where $M$ is the number of scattering sites and $N$ an integer. For the even and odd curves shown, we use the lowest $M$ for each group. $I_0 = (\hbar^2 M)/(2m_e\Phi_0)$. The two odd groups are in superposition at zero flux and the zone boundary, while the even groups only have a single flux value for superposition. There is a half period flux shift between the superposition for the even $4N$ (zero flux) and $4N + 2$ (zone boundary), as well as the odd $4N + 1$ and $4N + 3$ (min/max switched) groups. We have described these relations in the past.[21,22]

of external readout measurement (external coupling), which is supposed to collapse the wavefunction of the network to provide a classical result, does not need to be weak or brief. In fact strong and permanent external perturbation to the isolated and entangled AB rings is desirable for a robust readout, provided that the strength of the entanglement is stronger in cooperation with the external perturbation.

The half-adder computing capability from two coupled AB rings is clear. The four angular momentum pairings can be mapped into the four rules for addition of two binary values: 00, 01, 10, and 11. Here, the 00 pair indicates the angular momenta of the two AB rings are both CW, and so on. This mapping can be arbitrarily assigned and evaluated with flux values of the same magnitude. Such a circuit has been shown recently by us.[23] The classical readout requires a test signal (an input) to sample through the two coupled AB rings and the results (the outputs), namely "sum" and "carry," need to be correctly separated. That requires two terminals alone. Furthermore, an additional third terminal is needed when the 00 operation case arises, since the Boolean rules require the test signal not to reach the "sum" or "carry" terminals. Hence, it must appear on the extra third terminal. Thus, a half-adder is composed of a simple structure of two coupled AB rings with three attached external terminals for readouts, which is further characterized in Sec. III A. Such a half-adder replaces between one and two dozen MOSFET transistors (depending on static or dynamic implementation) used in current classical circuits. More broadly in Sec. III, we examine how weak and strong external perturbations affect the readout from a quantum computing scheme that is implemented.

The demonstration of electron transmission through an AB ring with two strongly coupled terminals was shown in the mid-1980s.[24] This is the simplest form of a quantum network connected to two chemical potential reservoirs. Even in this form, there are three classes of electron transmission, depending on the locations of the two terminals and the total number of atoms (sites) in the ring. Each class is like a fundamental mode of a microwave waveguide. There is further a scaling relation where a properly scaled up version of the ring will exhibit an identical transmission to its smallest possible atomic sized ring.[21] Generalization of such quantum networks to three and four terminals have been investigated for possible wave-computing using the vector sum of two coherent inputs.[25,26]

Recently, we tried to relate the qubit-concept based computing through a quantum network-based framework. We showed that with three such strongly perturbed external leads, a high-fidelity classical sequential readout is possible. In this paper, we will further show (I) how weak and strong entanglements along with (II) how weak and strong external perturbations will affect the result for a classical readout separately. Our investigation of these quantum networks is based on an exact and non-tight-binding global node equation method formulated previously by one of these authors, and can be reviewed in the literature.[21] Finally, we summarize the differences between mainstream qubit-based computing and the approach for quantum networks in Sec. IV.

## II. ANGULAR MOMENTUM ENTANGLEMENT IN QUANTUM NETWORKS

If two AB rings are entangled together in a very weak manner, such as by quantum point contact, then each loop can be treated as their own Hilbert spaces. This leads to four possible system states $|A_{loop}\rangle \otimes |B_{loop}\rangle$ and is illustrated in Fig. 2(a) where the persistent current of the pair behaves similarly to that of a single AB ring shown in Fig. 1, with superpositions exhibited at $\Phi = 0$, $\pm 0.5\Phi_0$, $\pm\Phi_0$, and so on. Therefore with a point contact entanglement, the qubit model is still valid for any combination of input fluxes.

Generally when two AB rings are touching one another, there is an entanglement or overlapping of the partial wavefunctions of the two rings. When two AB rings are point-contacted (Fig. 2(a)), this is a minimum entanglement where a superposition of the four states exists because the energy spectrum remains the same as that of a single AB ring. As two rings become closer, the overlapping is increased and there is a common path (one or two channels) such that the phase of the wavefunction can be modulated by two independent fluxes (Fig. 2(b)). This increases the degree of entanglement and is reflected by the lowering of the Fermi

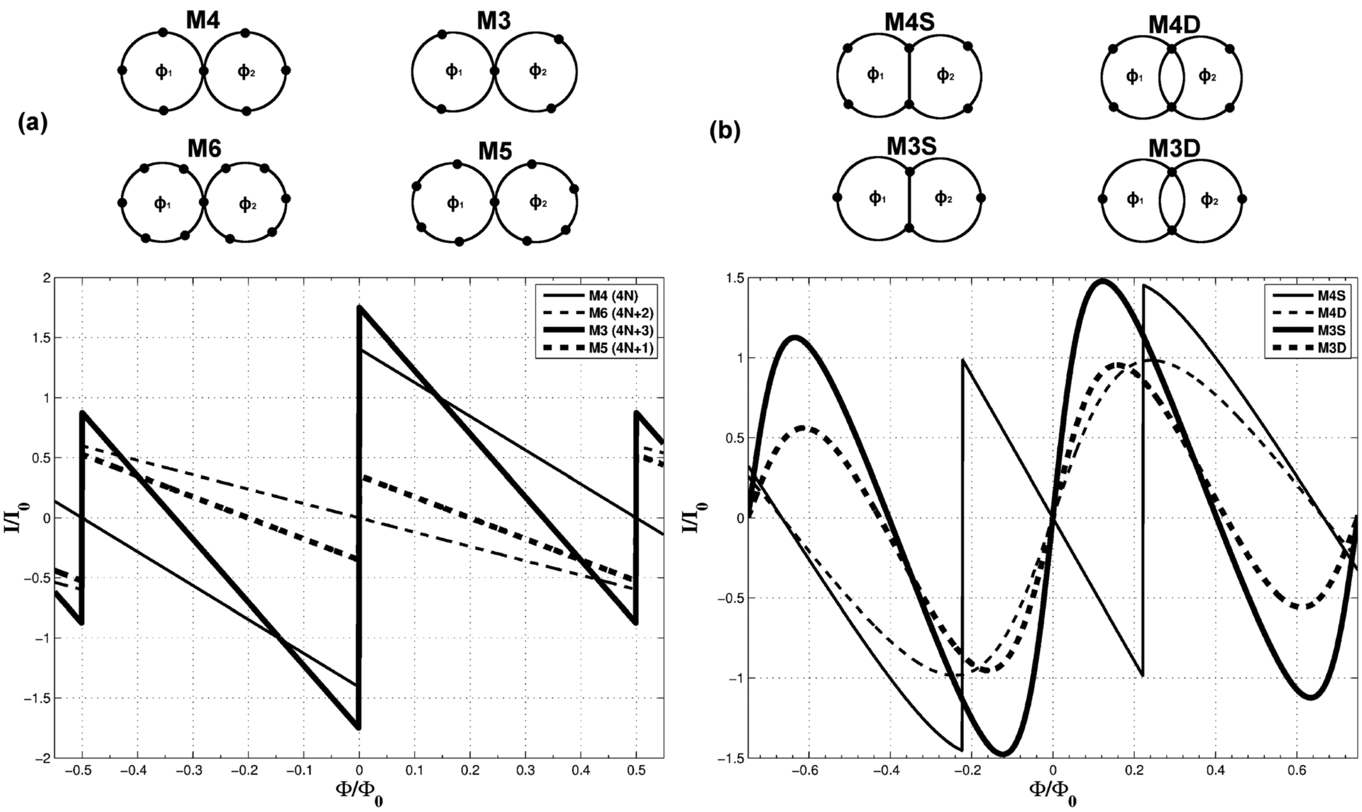


FIG. 2. Change of superposition capability as the strength of entanglement increases. (a) Weak entanglement of the four possible groups for even and odd AB rings, coupled by a single scattering site (point contact rings). The superposition is preserved due to the band structure being unaltered from the single ring. (b) Strong entanglement for the two smallest even/odd groups ($4N$, $4N+3$), either with a single center common path (S) or a double (D). Generally, the superposition is destroyed, but single bonds which represent the strongest entanglement in quantum networks can overlap the band states at $E_f$ to a degree that also produces a superposition (as in M4S). The applied fluxes are given as $\Phi = \phi_1 = \phi_2$. Note that the other two groups ($4N+2$, $4N+1$) need not be investigated due to scaling laws we have noted earlier. Thus they will behave qualitatively similar to that of their respective sister group, though with a possible flux shift.

level, $E_f$, with the overlap of bonding states being pulled up, and the anti-bonding states being pulled down, respectively, in energy space at one flux period. In isolated coupled AB networks that only share a middle common path (or two), the entanglement is much stronger with a broadened flux periodicity (dependent upon the geometry of the network), as given by Eqs. (6) and (7) in Ref. 23. The entanglement is considered at its strongest when there is only a single common path, shown in the upper-left of Fig. 2(b). When the entanglement becomes this strong, the bonding and anti-bonding states can be at equal energy for certain flux values within the first Brillouin zone and when the applied fluxes to the loops are equal in magnitude.[22] At these Fermi level crossing points between states, there is an inherent uncertainty in the direction of the persistent current flowing in the network (hence in a superposition), at $|\Phi| = \frac{2}{9}\Phi_0$. Superposition is also observed for single AB loops with no applied flux, which was outlined in Sec. I (Fig. 1). It is important to note that for entanglements stronger than a point contact situation, this Fermi level crossover behavior is only observed in even-numbered rings (either groups $M = 4N$ or $4N + 2$ due to scaling laws) that are coupled by a single path (the strongest form). Since the charge density within the common path is either zero at its midpoint or its divergence is,[22] the portions of the persistent current in both rings must be flowing in the same direction of the angular momentum. Physically, if one were to measure the current for one loop, there would be no guarantee of a given direction. However, whatever the outcome for the first loop, the second loop's measurement is guaranteed to be identical with the first. This is true even for Fermi level crossings and at the zone boundary. Therefore, the state of the system can be described by two Bell states

$$|\Psi\rangle = \alpha|\psi^+\rangle + \beta|\psi^-\rangle, \tag{2}$$

where $|\psi^+\rangle = \frac{1}{\sqrt{2}}(|00\rangle + |11\rangle)$ and $|\psi^-\rangle = \frac{1}{\sqrt{2}}(|00\rangle - |11\rangle)$. It is clear that as the degree of entanglement between the coupled rings increases past the point contact stage, there is no guarantee anymore of preserving all four possible states. We show that the ring-to-ring interaction destroys the superposition for the weaker double bond couplings, while moving to maximum entanglement (singe bond) will intuitively produce a Bell situation, though only for networks that fall into an even-numbered classification group. This provides a contrast with qubit-based quantum computing, where superposition is assumed during entanglement. Quantum computing at a minimum must be able to perform the algebraic operations first.

## III. EXTERNAL COUPLING STRENGTH CONSIDERATION

In qubit-based quantum computing, the typical approach is to attempt to determine the state of the system without

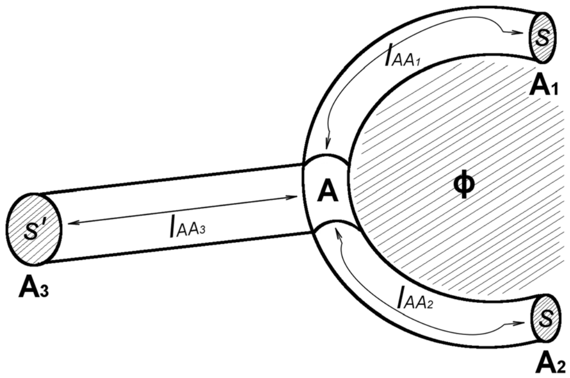


FIG. 3. Lattice-structured quantum network which forms the basis for the global node equation method. The boundary condition for conservation of momentum at A allows us to form a linear set of equations describing the stationary states at each of the scattering sites.

disturbing the internal state or superposition, meaning a closed system basically. In other words, for a readout a weak or indirect measurement is necessary. In the quantum network approach, external perturbations for readouts are typically permanently attached and strong. In this section, we describe how varying the external coupling strengths for both weak and strong entangled quantum rings can affect the readout of the computations. We denote the external perturbation strength with the coupling parameter $\Delta$, which is the cross-sectional area ratio of the terminal probe to the electron waveguides of the ring itself. In the global node equation approach we have used in our calculations, $\Delta$ can be derived for an intersection site A connected to three other scattering sites (labeled $A_{1-3}$) by leads of a single lattice spacing as (see Fig. 3)

$$\begin{aligned} s_1\Psi(A_1)\csc kl_{AA_1} &= s_1\Psi(A)[\cot kl_{AA_1} - \tan\delta_{AA_1}]e^{-i\theta_{AA_1}},\\ s_2\Psi(A_2)\csc kl_{AA_2} &= s_2\Psi(A)[\cot kl_{AA_2} - \tan\delta_{AA_2}]e^{-i\theta_{AA_2}},\\ s_3\Psi(A_3)\csc kl_{AA_3} &= s_3\Psi(A)[\cot kl_{AA_3} - \tan\delta_{AA_3}]e^{-i\theta_{AA_3}}, \end{aligned} \tag{3}$$

where cross sections $s_1 = s_2 = s$, $s_3 = s'$, lengths $l_{AA_1} = l_{AA_2} = l_{AA_3} = l$, and phase factor $\theta_{AA_j} = \frac{1}{\Phi_0}\int_0^l \mathbf{A}(x')\cdot d\mathbf{x}'$. Satisfying conservation of current, $\sum_{j=1}^{3}\tan\delta_{AA_j} = 0$, with $\tan\delta_{AA_j} = i\frac{C_{AA_j} - D_{AA_j}}{C_{AA_j} + D_{AA_j}}$, where C and D are the outgoing and

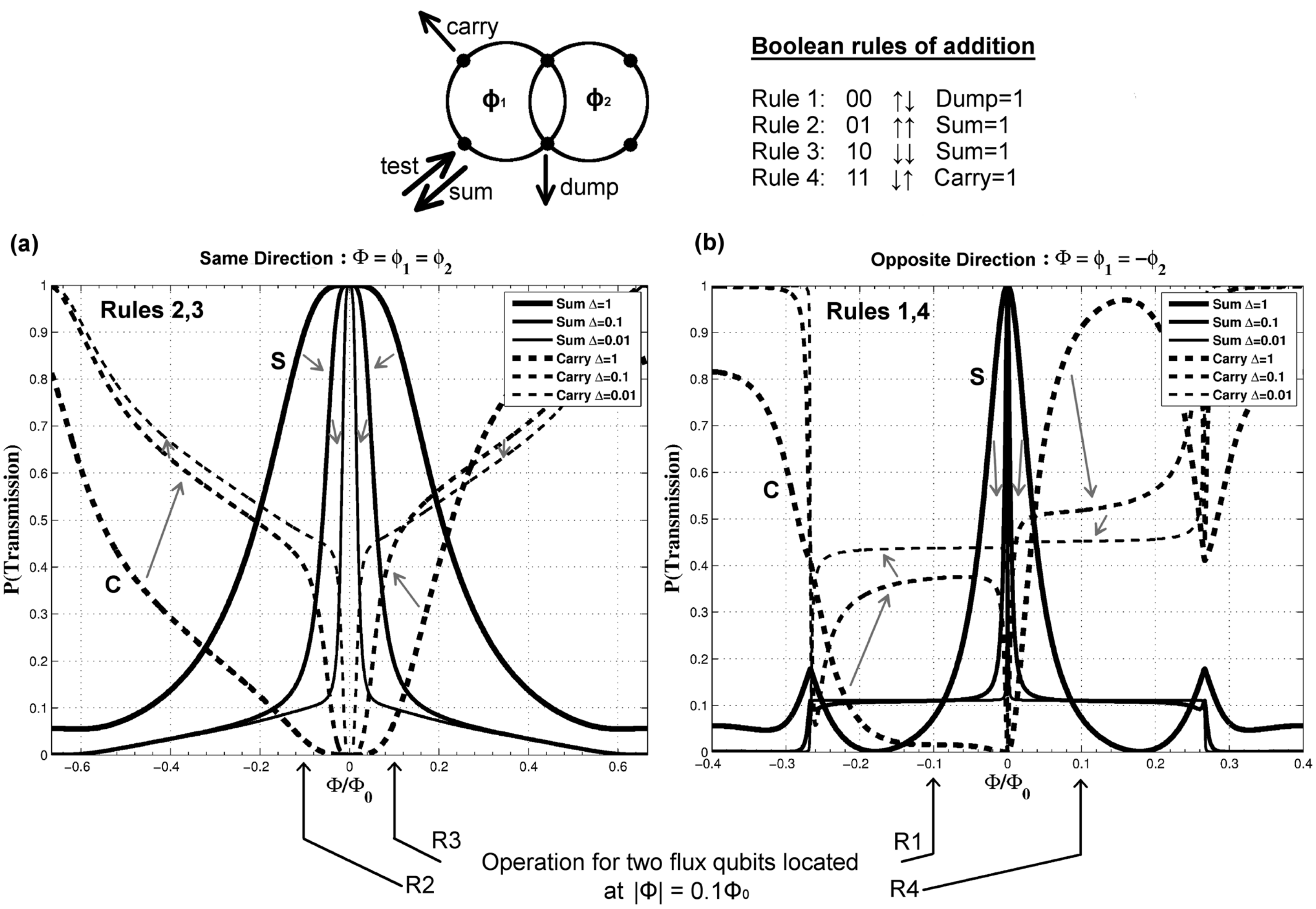


FIG. 4. Two strongly coupled AB rings, beyond the point-contact situation, is shown in the upper figures. When $\phi_1 = \phi_2 = \pm 0.1\Phi_0$ in (a), a test signal from the sum terminal, results in a total reflection, so that the output at the sum terminal $\approx 0.9$, while the carry terminal output $\approx 0.1$. The two results are mapped into the Boolean algebra rules of addition for two bits 1 and 0. This is shown in the bold solid curve when $\Delta = 1$ (strong external coupling). The grayscale arrows indicate the progression as the coupling is reduced. When $\Delta$ is reduced, the results are no longer valid because the sum/carry relation changes into different, less distinguishable modes ($\Delta = 0.1$ and 0.01). In (b) when $\phi_1 = -\phi_2 = 0.1\Phi_0$, the carry terminal $\approx 0.9$, while the sum terminal $\approx 0.1$. This maps into the Boolean algebra rules of addition for two bits 1 and 1. On the other hand when $\phi_1 = -\phi_2 = -0.1\Phi_0$, both carry and sum terminals are low, and the output goes to the third dump terminal (not shown). This maps into the addition for two bits 0 and 0. The above statement is valid only at $\Delta = 1$, the maximum external coupling situation. When $\Delta$ is reduced to 0.1 or 0.01, the results are not valid as shown in the dotted curves. Thus a workable half-adder we have shown here has uniform cross-sectional area throughout the rings and the external leads.

incoming amplitudes along path $AA_j$, respectively. If the external terminal is connected along the non flux-modulated path $l_{AA_3}$ then $\theta_{AA_3} = 0$ and we can define $\Delta = \frac{s'}{s}$. Rewriting the localized linear set of equations in homogeneous form gives

$$\Psi(A)[2\cot kl + \Delta \tan \delta_{AA_3}] - \csc kl \sum_{j=1}^{2} e^{i\theta_{AA_j}} \Psi(A_j) = 0. \quad (4)$$

This is equivalent to the traditional S-matrix formulation shown by Büttiker *et al.*[27] Note that $\Delta = 1$ corresponds to maximum coupling, while $\Delta = 0$ describes the isolated unperturbed rings. If this approach is globally extended to each scattering site in the network, a secular equation can be formed for the eigenenergies that will lead to the calculations of the reflection and transmission amplitudes of the test signal for given terminal sites.[23]

## A. Strong entanglement with varying external perturbation strengths

It is possible to construct a half-adder circuit with two AB rings entangled by two shared center bond lengths, where all four pairing states can be satisfied classifically. This network presumes a strong and permanent perturbation or $\Delta = 1$. Quantum networks are understood to be of a waveguide nature. We have shown previously how a test signal can be transported through multiple-terminal networks.[22,23,25,26] Transport with a test signal for a three-terminal network can be generally divided into three primary classes: dominant, half-sharing, or equal-sharing between the output terminals. From the truth table for a half-adder, it is simple to see that only a single output should be $|1\rangle$ for any given flux combination. Therefore, a dominant class of transport is favorable for this form of computation. From our calculations, we see that if the coupling parameter between the external terminals and the rings begins to weaken, then the transport classification begins to change. The domination for the sum and carry terminals begins to be weakened slowly into a more distributed class. Therefore, the ability to take a high-fidelity measurement of the computation through the test signal is absent at weak coupling parameters, leaving indistinguishable readout results. This is shown in Fig. 4.

## B. Weak entanglement with varying external perturbation strengths

In Fig. 2(a), we show that for point-contact coupled AB loops, superposition of states exist at $|\Phi| = \frac{1}{2}\Phi_0$ and 0. This is the situation for a weakest entanglement. The question is whether this can be accompanied by a weak external perturbation to provide a classical readout. For comparison, we investigated the two weakest entangled AB rings, where superposition of all four states exists before the attachment of external terminals. Since there is no shared center path between the two partial waves in each ring, the eigenenergies remain unchanged for applied fluxes $\phi_1 = \pm\phi_2$. This is due to the associated secular equation only having flux terms contained within cosines.[23] The result is that the electron transport is sign-invariant for one of the fluxes, and thus there are only two possible electron wavefunction output vectors in the weakest entanglement, instead of four. For half-adder addition, this is not desirable since there needs to be a total of three distinct output states. The results are shown in Fig. 5. For the class of point-contacted AB rings, with an odd number of atoms in each ring, labeled as M3, we found a gradual transport trend. The two output states are slowly degraded from dominant transport at one terminal to a more distributed situation. For the second class of two even point-contacted rings, M4, the test signal is completely reflected across the entire flux period for all non-zero coupling strengths (not shown), and is therefore not useful for computation. In summary, lowering the coupling strength between the external terminals and the network will generally degrade the readouts to such a point where the computation can no longer be reliably found or distinguished. Therefore there is no possibility of a classical readout, even though the unperturbed coupled rings can exhibit a superposition of states. This is because superposition of states holds true only in a closed system, while readout possibility is from an open system only. In special cases where there is total reflection of a test signal across the entire first Brillouin

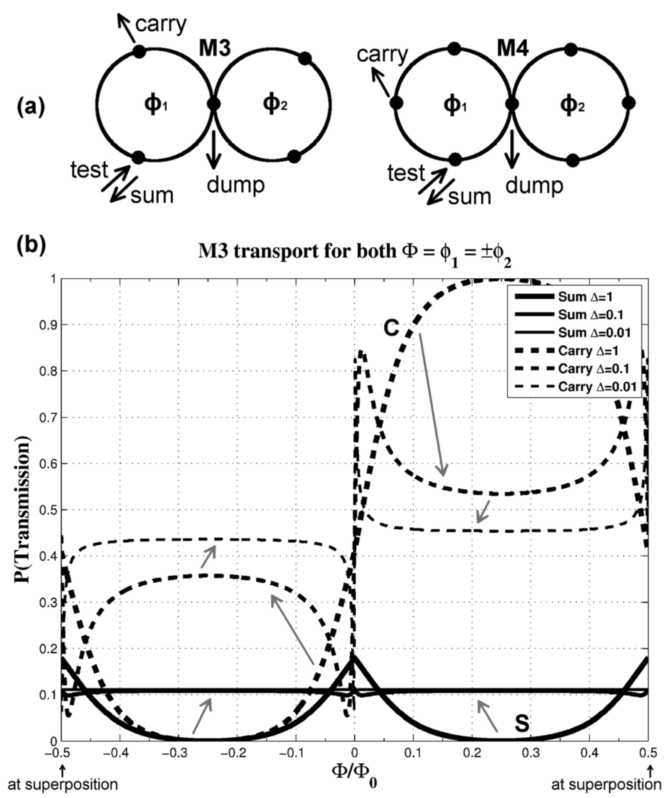


FIG. 5. Weak entanglement versions of the half adder circuit. (a) Odd M3 and even M4 point-contact circuits. (b) M3 point-contact network transport as external terminal coupling is varied. The grayscale arrows indicate the progression as the coupling is reduced. The third (dump) terminal in our original work is not shown, since it only collects unwanted computations. Note that the results are for all four equal-magnitude angular momentum pairings, since the transport is sign-invariant for $\phi_2$. In $\Delta = 1$ situation, it behaves like a quantum circulator.[25] As external terminals are weakened, the transport approaches equal-distribution between the carry and dump (not shown). Note the flux period for point-contact entanglements are the same as for a single ring, $\Phi = \Phi_0$.

zone, this does not hold true as changes in coupling strength have no effect on the output.

## IV. CONCLUSIONS

In this paper, we show that as long as a single qubit, which is angular momentum based, can be established in a man-made atom or an AB ring, quantum computing can be made without the need to check the extent of entanglement for superpositional flux qubits in order to guarantee the classical readouts. The superposition nature of such networks is due to the fact that electron wavefunctions are composed of coupled harmonic oscillators (in the global node equation) in an AB ring, and hence at the Brillouin zone boundary a switching of the direction of the angular momentum can occur. Therefore, the subsequent constructions for the entanglement of two coupled AB rings to serve as a half-adder circuit as well as the required setup for a classical readout do not necessarily follow the procedures outlined by earlier investigators. The existence of a superposition for qubits has long been assumed when there is entanglement. This is required strictly for a closed system only. However, our results lead us to believe that superposition of states may not be needed for classical readout results because the readouts require an open system. Our findings point out that there is an interplay between the entanglement (internal coupling) and the external perturbation configuration (external coupling). The entanglement can be provided in such a way that there is a loss of superposition, while the external connections are attached. We show indeed that classical readouts are possible at the loss of superposition. The conventional wisdom of having a perfect internal quantum computation scheme first (closed system) and then reading the result with weak or indirect measurement, in order to keep the system closed, turn out not to be valid in our quantum network example shown here, and therefore is necessarily not valid in the general situation. In general, attempting to sample a closed quantum network in a superposition with a test signal results in a rejection of the probes with complete reflection. We have shown that strong external perturbations can provide high-fidelity classical readouts, while weak perturbations generally switch the quantum circuit from one class (dominant output) to another weaker (distributed output) class that cannot provide any useful readouts. In quantum computing, as long as it is qubit-based at the start, the internal couplings of qubits (the entanglement) and the external couplings for collapsing the internal quantum state to a classical distribution (the setup for readouts) are one integral part of a circuit that cannot be considered separately. For robust classical measurements, a strong external perturbation must be paired with a strong enough entanglement that can destroy the superposition of the two qubits. Any other combination of external and internal couplings will not lead to this desired computational output behavior.

While qubit-based quantum computing is shown to be able to perform so called "massive parallel computing" as shown by Shor's algorithm[28] for fast factorization, a fundamental problem still exists at the very elementary level of simply adding two n-bit binary strings together. This is analogous to performing the Fourier transform in optical computing,[29] which is a special case that a single lens gate can solve in parallel. However, this in no way implies that such parallelism can be extended to general arithmetic logic operations that depend on addition-based Boolean algebra. In quantum network theory, we show one possibility to integrate a quantum algorithm with strong external perturbations so that high-fidelity classical measurement is possible. In our scheme, superposition of angular momentum states can exist in a closed system fashion, but needs to be collapsed in coordination with the readout configuration in an open system. The coordination scheme we have demonstrated is to strengthen the internal coupling, at a loss of superposition with the attachment of strong externally coupled terminals to form said open system. Any other combination will not provide meaningful readout results in our model. In summary, a closed system has been transformed into an open and useful system.


[1]D. P. DiVincenzo, Fortschr. Phys. **48**, 771 (2000).
[2]D. Loss and D. P. DiVincenzo, Phys. Rev. A **57**, 120 (1998).
[3]G. Burkard, D. Loss, and D. P. DiVincenzo, Phys. Rev. B **59**, 2070 (1999).
[4]S. A. Wolf, D. D. Awschalom, R. A. Buhrman, J. M. Daughton, S. von Molnár, M. L. Roukes, A. Y. Chtchelkanova, and D. M. Treger, Science **294**, 1488 (2001).
[5]A. Imamoglu, D. D. Awschalom, G. Burkard, D. P. DiVincenzo, D. Loss, M. Sherwin, and A. Small, Phys. Rev. Lett. **83**, 4204 (1999).
[6]D. D. Awschalom and M. E. Flatte, Nat. Phys. **3**, 153 (2007).
[7]M. D. Reed, L. DiCarlo, S. E. Nigg, L. Sun, L. Frunzio, S. M. Girvin, and R. J. Schoelkopf, Nature **482**, 382 (2012).
[8]T. Meunier, V. E. Calado, and L. M. K. Vandersypen, Phys. Rev. B **83**, 121403 (2011).
[9]R. Hanson and D. D. Awschalom, Nature **453**, 1043 (2008).
[10]R. Hanson and G. Burkard, Phys. Rev. Lett. **98**, 050502 (2007).
[11]R. Hanson, F. M. Mendoza, R. J. Epstein, and D. D. Awschalom, Phys. Rev. Lett. **97**, 087601 (2006).
[12]J. M. Elzerman, R. Hanson, J. S. Greidanus, L. H. Willems van Beveren, S. De Franceschi, L. M. K. Vandersypen, S. Tarucha, and L. P. Kouwenhoven, Phys. Rev. B **67**, 161308 (2003).
[13]L. DiCarlo, J. M. Chow, J. M. Gambetta, Lev S. Bishop, B. R. Johnson, D. I. Schuster, J. Majer, A. Blais, L. Frunzio, S. M. Girvin, and R. J. Schoelkopf, Nature **460**, 240 (2009).
[14]L. DiCarlo, M. D. Reed, L. Sun, B. R. Johnson, J. M. Chow, J. M. Gambetta, L. Frunzio, S. M. Girvin, M. H. Devoret, and R. J. Schoelkopf, Nature **467**, 574 (2010).
[15]N. C. Jones, R. Van Meter, A. G. Fowler, P. L. McMahon, J. Kim, T. D. Ladd, and Y. Yamamoto, Phys. Rev. **X2**, 031007 (2012).
[16]L. Pauling, J. Chem. Phys. **4**, 673 (1936).
[17]C. A. Coulson, Proc. Phys. Soc. A **67**, 608 (1954).
[18]K. Ruedenberg and C. W. Sherr, J. Chem. Phys. **21**, 1565 (1953).
[19]S. A. M. Weger and G. D. Riccia, J. Math. Phys. **14**, 259 (1973).
[20]E. Montroll, J. Math. Phys. **11**, 635 (1970).
[21]C. H. Wu and G. Mahler, Phys. Rev. B **43**, 5012 (1991).
[22]L. T. C. H. Wu and C. A. Cain, J. Appl. Phys. **111**, 094304 (2012).
[23]C. A. Cain and C. H. Wu, J. Appl. Phys. **110**, 054315 (2011).
[24]R. A. Webb, S. Washburn, C. P. Umbach, and R. B. Laibowitz, Phys. Rev. Lett. **54**, 2696 (1985).
[25]C. H. Wu and D. Ramamurthy, Phys. Rev. B **65**, 075313 (2002).
[26]D. Ramamurthy and C. H. Wu, Phys. Rev. B **66**, 115307 (2002).
[27]M. Büttiker, Y. Imry, and M. Y. Azbel, Phys. Rev. A **30**, 1982 (1984).
[28]P. W. Shor, SIAM J. Comput. **26**, 1484 (1997).
[29]A. D. McAulay, *Optical Computer Architectures* (Wiley New York, 1991).